Analytica Chimica Acta 1167 (2021) 338570

Contents lists available at ScienceDirect

Analytica Chimica Acta

journal homepage: www.elsevier.com/locate/aca

Reproducible, shelf-stable, and bioaffinity SERS nanotags inspired by multivariate polyphenolic chemistry for bacterial identification

Lunjie Huang [a, b, c], Da-Wen Sun [a, b, c, d, *], Zhihui Wu [a, b, c], Hongbin Pu [a, b, c], Qingyi Wei [a, b, c]

[a] School of Food Science and Engineering, South China University of Technology, Guangzhou 510641, China
[b] Academy of Contemporary Food Engineering, South China University of Technology, Guangzhou Higher Education Mega Center, Guangzhou 510006, China
[c] Engineering and Technological Research Centre of Guangdong Province on Intelligent Sensing and Process Control of Cold Chain Foods, & Guangdong Province Engineering Laboratory for Intelligent Cold Chain Logistics Equipment for Agricultural Products, Guangzhou Higher Education Mega Centre, Guangzhou 510006, China
[d] Food Refrigeration and Computerized Food Technology (FRCFT), Agriculture and Food Science Centre, University College Dublin, National University of Ireland, Belfield, Dublin 4, Ireland

HIGHLIGHTS

- Polyphenolic chemistry enabled from-synthesis-to-bioaffinity scheme of SERS tags.
- Metal-phenolic networks acted as bioaffinity elements for bacterial recognition.
- Polyphenolic SERS tags could be reliable detection probe for bacteria quantitation.
- Polyphenolic SERS biosensor could detect foodborne bacteria down to 10^2 CFU/mL.
- The SERS biosensor could work in milk and beef samples.

GRAPHICAL ABSTRACT

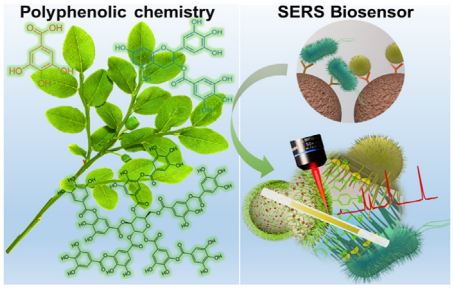

ARTICLE INFO

Article history:
Received 12 January 2021
Received in revised form
26 March 2021
Accepted 21 April 2021
Available online 28 April 2021

Keywords:
Foodborne pathogens
Microbial food safety
Metal-phenolic networks
Polyphenols
SERS detection

ABSTRACT

Efficient identification of pathogenic bacteria is greatly concerned with microbial food safety and foodborne diseases diagnosis. Surface-enhanced Raman scattering (SERS) tags are among the cutting-edge tools for bioanalysis, but facing troubles in either SERS sensitivity, durability, interfering signals, or universal recognition agents for target bacteria. This work proposed a multivariate scheme enabled by polyphenolic chemistry for the green synthesis, facile stabilization (functionalization), protective encapsulation, and bio-affinitive design of metal-phenolic networks (MPNs)-encapsulated silver SERS nanotags (AgNPs@4-mercaptobenzonitrile@MPNs). With remarkable SERS properties, shelf stability, and bacterial affinity, AgNPs@4-mercaptobenzonitrile@MPNs tags enabled rapid, reproducible, and interference-free SERS detection of two representative foodborne pathogens (*i.e., E. coli* O157: H7 and *S. aureus*) in the assistance of an aptamer-labelled magnetic probe, reaching good sensitivity and selectivity. Moreover, this SERS biosensor worked well in real food samples, manifesting the potential of polyphenolic chemistry in the customization of bio-affinitive SERS nanotags for food safety detection.

* Corresponding author. School of Food Science and Engineering, South China University of Technology, Guangzhou 510641, China.
E-mail address: dawen.sun@ucd.ie (D.-W. Sun).

https://doi.org/10.1016/j.aca.2021.338570

1. Introduction

With the prevalence of COVID-19 epidemic, human society has paid unprecedented attention to microbial food safety among the global food trade system [1]. Consuming food contaminated by pathogenic bacteria or viral microorganisms can cause severe pathological symptoms in the human body. Therefore, numerous detection techniques have been developed for the screening of microbial risks in the food market, including traditional plate counting and polymerase chain reaction (PCR) methods, and optical [2,3], electrochemical [4], and biosensing methods [5,6]. Recent developments have potentiated methods for the rapid (from minutes to hours) and sensitive (single-cell level) identification of bacteria to fulfil increasing early diagnostic demands in the medical [7], agri-food [8], and environmental fields.. As an ultrasensitive vibrational spectroscopic technique, surface-enhanced Raman scattering (SERS) stands out for its excellent signal enhancement with an enhancement factor of 10^{6-9}, narrow and characteristic Raman fingerprints, and non-invasive and rapid spectral acquisition [9–17]. In particular, by combining the SERS effect of plasmonic nanoparticles and the Raman fingerprint of organic Raman reporter molecules (Scheme 1, fabrication procedures), SERS tags have been developed as a powerful bioanalytical tool for indirectly sensing/imaging various biochemical analytes [18–20], including small biomolecules, DNA sequences, proteins, cells, bacteria, and biological tissues [21]. In essence, SERS tags can exert optical labelling properties comparable to colourimetric/fluorescent chromophores, attaining ultrasensitive, quantitative, and multiplexing capabilities of the SERS technique.

Although further advancements in aforementioned SERS tag techniques for bacteria biosensing can be challenged by the following issues (Scheme 1, technical details): (1) synthesis of elegant metallic nanosubstrates [22–27], as silver nanoparticles (AgNPs) are generally more preferred due to its higher SERS, while AgNPs via typical synthesis rarely retain monodisperse uniformity and chemical stability; (2) signal sensitivity and reproducibility, which requires both a rational selection of Raman reporters and a preferential nanosubstrate surface for the adsorption of these reporters; (3) shelf durability of nanotags and background interferences, where an ideal scenario is that environmental effects can be eliminated by a protective coating without sacrificing signal intensity; (4) lack of efficient molecular affinity agents beyond antibodies/aptamers, limiting versatile recognition patterns for bacteria. For overcoming these challenges, on one hand, recent efforts have been devoted to promoting sensing performance of SERS tags, including (a) optimizations in synthesis and stabilization for AgNPs [28–32], (b) adoption of Raman reporter molecules with anti-interference properties (such as peaks located in so-called "Raman-silent region" of 1800–2800 cm^{-1}) to silence background noises [33], and (c) surface engineering of nanosubstrates via functional groups or inorganic/organic shells to shield environmental influences[34–37]. However, there are few successful examples in achieving highly stable, reproducible, and interference-free silver SERS nanotags. On the other hand, a large number of molecular recognition elements have been screened out for integrated bacteria sensing [38–40], such as small molecules [41–43], antibiotics [44], peptides and proteins [45], or positively charged nanomaterials [46,47]. However, it is often troublesome and challenging to efficiently integrate these recognizers with SERS tags. Moreover, none of the studies available has taken into account the above issues in combination, remaining largely limited performance of the as-obtained SERS tags.

Polyphenolic compounds are abundant in natural species and versatile in chemical properties. Especially, with the emergence of

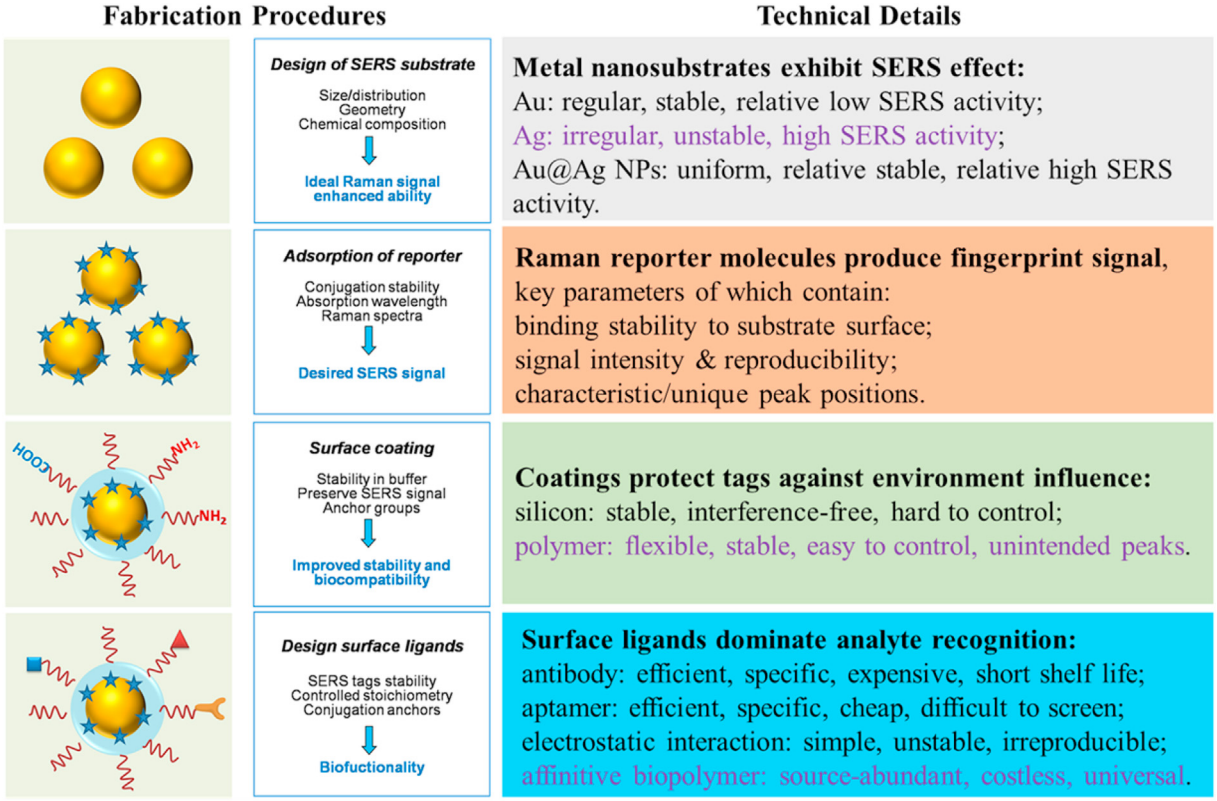

Scheme 1. Typical fabrication procedures and technical details for the design of SERS tags (adapted with permission [18]. Copyright 2013, American Chemical Society).

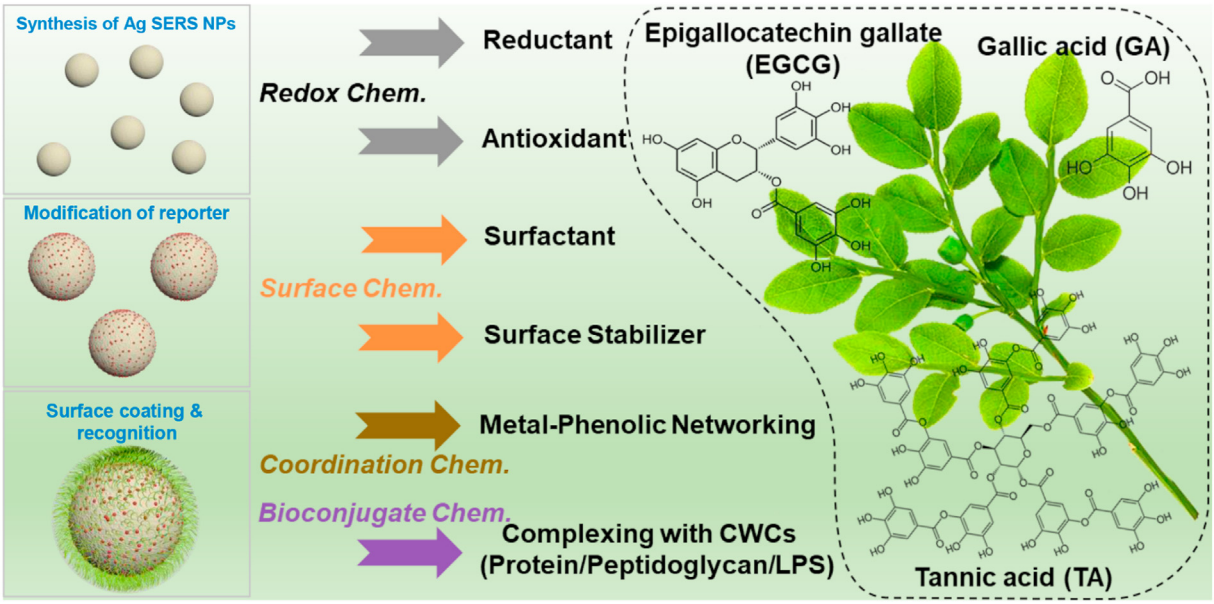

Scheme 2. The principle of polyphenolic chemistry for the synthesis, stabilization, modification, and functional design of silver SERS tags. Abbreviation: CWCs = cell wall components, and LPS = lipopolysaccharide.

metal-phenolic networks (MPNs) [48], polyphenols and their derivatives have become increasingly important scaffolds in the synthesis, functionalization, and surface modification of functional nanomaterials. Meanwhile, polyphenols have been applied for antibacterial applications [49,50], bacterial staining [51], and protein isolation [52] for a long time. More interestingly, from a viewpoint of molecular interactions, increasing studies have indicated that possible biochemical interactions exist between polyphenolic species and bacterial cell wall components (CWCs), *e.g.*, lipopolysaccharides [53], peptidoglycans, membrane proteins [54], and lipids [55], as well as analogue biomolecules [56]. These interactions imply a possible recognition of bacteria via polyphenol-guided affinity to bacterial CWCs. While polyphenols have been used for synthesizing SERS NPs, the utilization of polyphenolic chemistry to boost specific SERS bioanalysis via an integrated from-fabrication-to-multifunctionalization strategy has never been reported.

Inspired by the polyphenolic chemistry (*e.g.*, redox chemistry, surface chemistry, coordination chemistry, and bioconjugate chemistry), this work proposed a multivariate design of bio-recognition SERS nanotags from aspects including green preparation, facile modification, rapid stabilization, and bacterial bio-targeting. The as-obtained SERS nanotags, namely MPNs-encapsulated 4-mercaptobenzonitrile (4-MB) modified AgNPs (AgNPs@4-MB@MPNs), were examined with respect to SERS sensitivity, reproducibility, anti-interference ability, and shelf durability. More importantly, the viable binding affinity of MPNs towards bacteria was investigated and verified for the first time. Combined with an aptamer-modified magnetic capture probe, these polyphenolic nanotags demonstrated a fast, reproducible, and reliable quantification of typical foodborne bacteria. The application of this biosensor in real food samples was also examined in the current study.

2. Experimental

2.1. Reagents and materials

Foodborne bacterial strains, including *Escherichia coli* O157: H7 (*E. coli* O157: H7, ATCC700728), *Staphylococcus aureus* (*S. aureus*, ATCC6538), *E. coli* (ATCC22922), and *Salmonella enterica serovar Typhimurium* (*S. enterica*, ATCC14028), were obtained from Guangdong Engineering and Technology Research and Development Center of Microbial Food Safety (Guangzhou, China). Silver nitrate ($AgNO_3$) and sodium carbonate (Na_2CO_3) were purchased from Sinopharm Chemical Reagent Co., Ltd. (Shanghai, China). Polyphenolic compounds including tannic acid (TA), epigallocatechin gallate (EGCG), and gallic acid (GA) were supplied by Macklin Biochemical Co., Ltd. (Shanghai, China). Iron (III) chloride hexahydrate ($FeCl_3 \cdot 6H_2O$), copper (II) nitrate trihydrate ($Cu(NO_3)_2 \cdot 3H_2O$), and Zirconium (IV) chloride ($ZrCl_4$) were acquired from Aladdin Bio-Chem Technology Co., Ltd. (Shanghai, China). The Raman reporter molecule 4-mercaptobenzonitrile (4-MB) was bought from Acmec Biochemical Co., Ltd. (Shanghai, China). The DNA oligonucleotides, 5′−NH_2−C6-CCG GAC GCT TAT GCC TTG CCA TCT ACA GAG CAG GTG TGA CGG-3' (*anti-E. coli* O157: H7 aptamer) [57] and 5′−NH_2−C6-GCA ATG GTA CGG TAC TTC CTC GGC ACG TTC TCA GTA GCG CTC GCT GGT CAT CCC ACA GCT ACG TCA AAA GTG CAC GCT ACT TTG CTA A-3' (*anti-S. aureus* aptamer) [58], were synthesized and purified by Sangon Biotech Co., Ltd. (Shanghai, China). Lipopolysaccharides (LPS) from *E. coli* 055: B5 and peptidoglycans (PG) from *Bacillus subtilis* or *S. aureus* were procured from Yuanye Bio-Technology Co., Ltd (Shanghai, China). The *N*-hydroxysulfosuccinimide sodium salt activated magnetic beads (NHS-MBs) and BeaverBeads Mag NHS Kit were obtained from BEAVER Biosciences Inc. (Suzhou, China). Milk and beef samples were purchased from a local supermarket (Guangzhou, China). Ultrapure water prepared by a Milli-Q system (Millipore Corp., Bedford, MA, USA) was used throughout this work.

2.2. Instruments

The UV−vis absorption spectra were measured with a spectrophotometer (UV-1800, Shimadzu Co., Kyoto, Japan). The scanning electron microscopy (SEM) images were obtained from a field emission scanning electron microscope (Carl Zeiss NTS GmbH, Oberkochen, Germany). The high-resolution transmission electron microscopy (TEM) images and elemental mapping images were

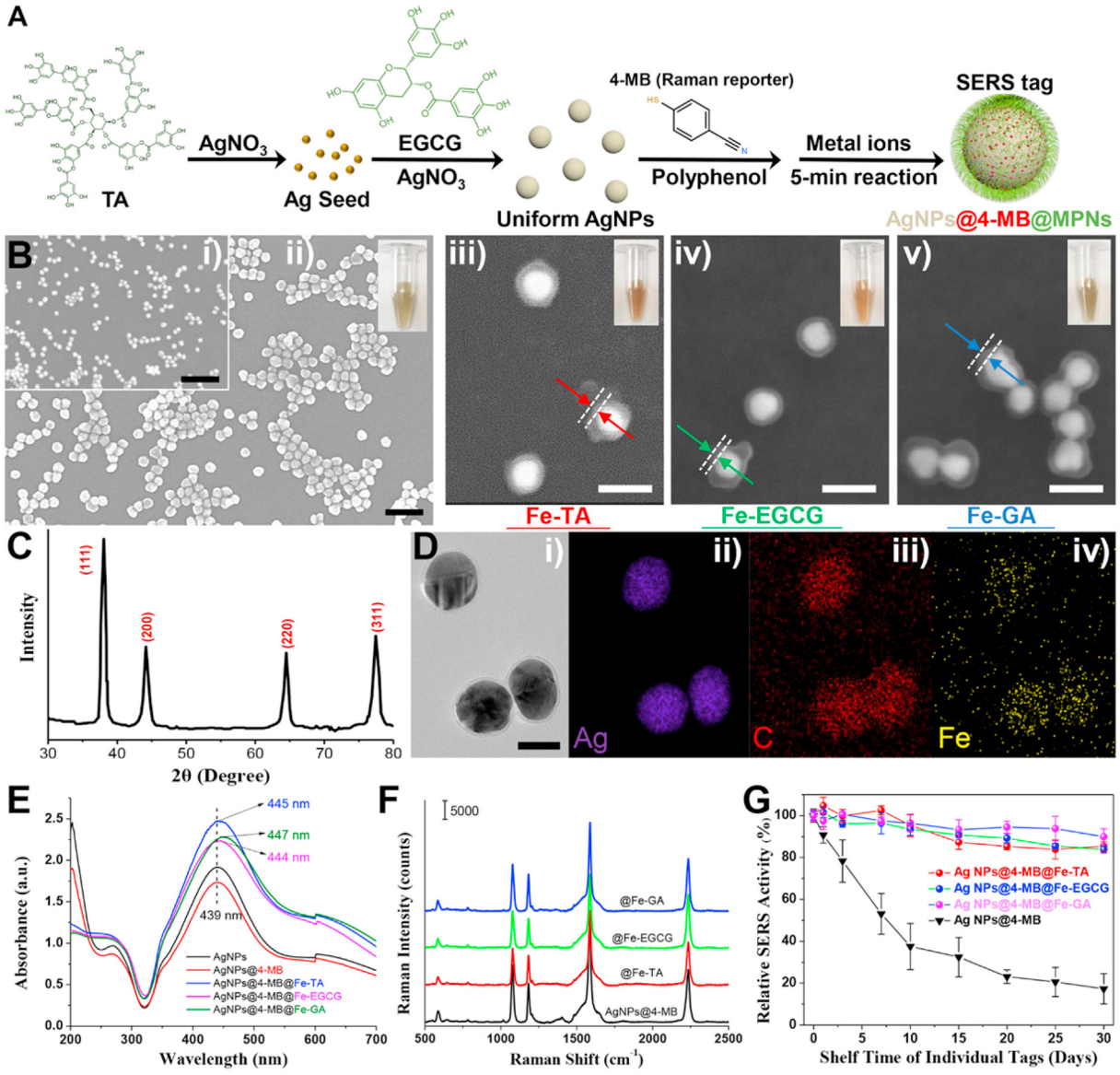

Fig. 1. (A) Schematic illustration of the green and rapid fabrication of MPNs coated silver SERS tags. (B) SEM images of (i) silver seeds, (ii) quasi-spherical AgNPs, scale bar = 200 nm; (iii -v) 4-MB modified AgNPs with coatings of (iii) Fe-TA, (iv) Fe-EGCG, and (v) Fe-GA MPNs, respectively. Scale bar = 100 nm. Insets are the optical images of the aqueous solutions of the corresponding NPs. (C) XRD pattern of AgNPs. (D) TEM image (i) and elemental distribution maps (ii-iv) of AgNPs@4-MB@Fe-TA. Scale bar = 50 nm. (E) The UV–vis spectra and (F) Raman characteristic spectra of the fabricated SERS tags. (G) The shelf life of individual SERS tags. The activities were evaluated by a characteristic peak at 2231 cm^{-1}. Condition: 532 nm laser (power: 12.5 mW), acquisition time of 5 s or 10 s for AgNPs@4-MB or AgNPs@4-MB@MPNs, respectively. (For interpretation of the references to colour in this figure legend, the reader is referred to the Web version of this article.)

taken from a JEM-2100F Plus high-resolution transmission electron microscope (JEOL Ltd., Tokyo, Japan) operating at an accelerating voltage of 200 kV. The X-ray diffraction (XRD) patterns of nanoparticles were acquired using an X-ray diffractometer (Empyrean, PANalytical B.V., Almelo, Netherlands). The zeta potentials were measured by a Zetasizer Nano ZS (Malvern Panalytical Ltd., Malvern, UK). The isothermal titration calorimetry (ITC) thermograms were collected from a calorimeter (MicroCal PEAQ-ITC, Malvern Panalytical Ltd., Malvern, UK), and analyzed with Malvern MicroCal PEAQ-ITC analysis software in a "one set of sites" fitting model. The SERS measurements were performed with a laser confocal Raman microscope system (LabRAM HR, Horiba France SAS, Villeneuve d'Ascq, France) equipped with a 10× objective lens and an air-cooled frequency-doubled Nd:YAG laser as the excitation source (532 nm, 50 mW). The acquisition time was 5–10 s with two accumulations.

2.3. Preparation of quasi-spherical Ag SERS NPs

The preparation of quasi-spherical AgNPs contains a two-step seed-growth reaction. For the synthesis of silver seeds, 100 μL of TA (4 wt%), 10 μL of Na_2CO_3 (0.5 M), and 200 μL of $AgNO_3$ (1 wt%) were added sequentially into 5 mL of the aqueous solution under constant shaking (IKA MS 3, IKA®-Werke GmbH & Co. KG, Staufen, Germany) with a centrifugation force of 1.6 *g*. After 1 h of reaction, the resulting dark brown silver seeds were washed for three times before redispersion in 1 mL water.

To obtain quasi-spherical AgNPs, 25 μL of the as-prepared Ag seeds were dispersed into 4.75 mL water, followed by the addition of 50 μL of $AgNO_3$ (1 wt%) and 200 μL of EGCG (10 mM) under

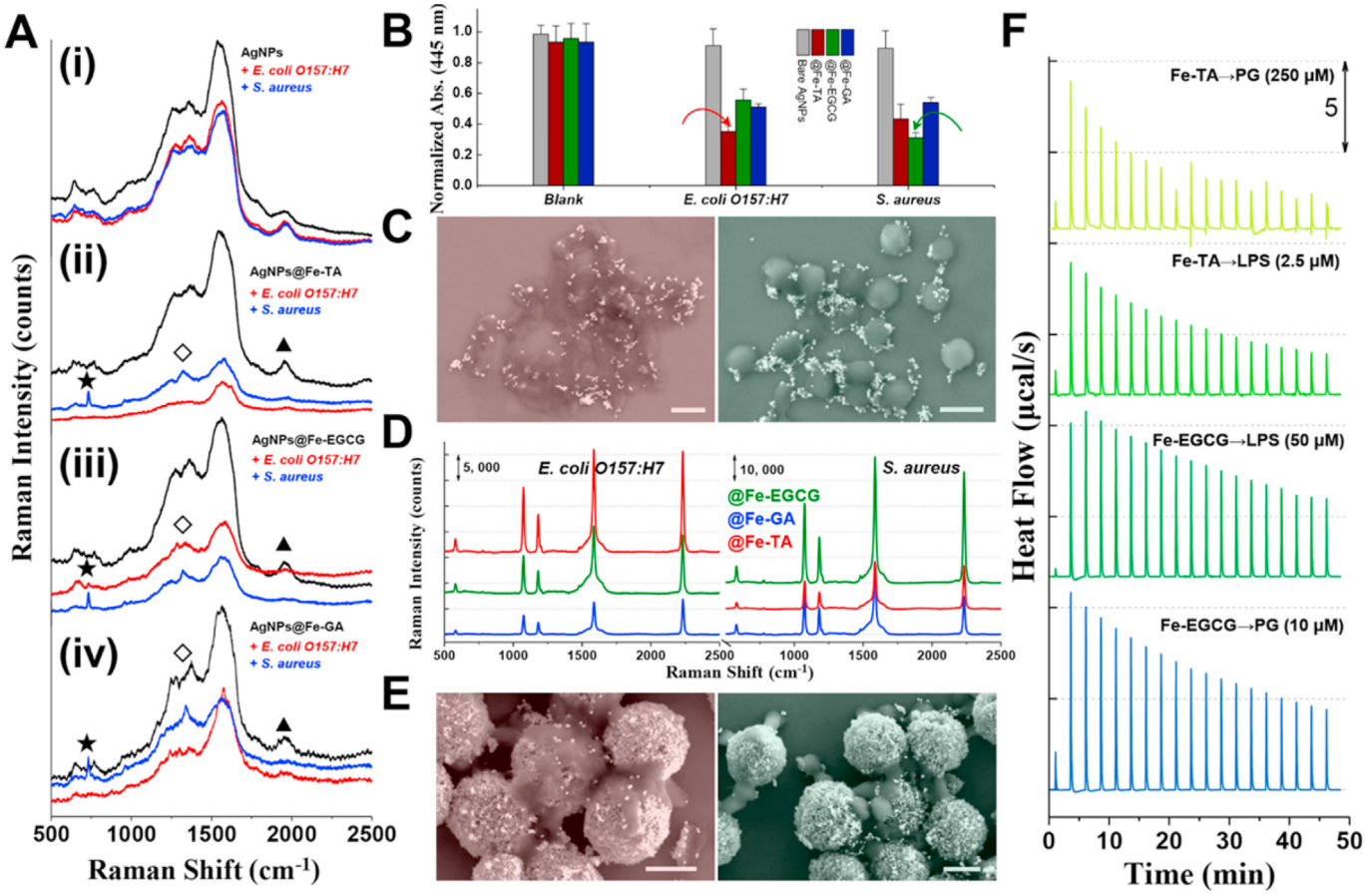

Fig. 2. (A) The Raman spectra of incubation solution of bacteria cells (10^6 CFU/mL) with (i) bare AgNPs, (ii) AgNPs@Fe-TA, (iii) AgNPs@Fe-EGCG, and (iv) AgNPs@Fe-TA, respectively. Condition: 2 h of incubation, measured with 532 nm laser (power: 12.5 mW), acquisition time 10s. (B) The binding performance towards *E. coli* O157: H7 and *S. aureus* for different SERS tags. Measured by absorbance changes at 455 nm of the filtration solutions (conducted with 0.22 μm syringe filters) after 2 h of incubation. (C) SEM images of the binding complexes of AgNPs@Fe-TA + *E. coli* O157: H7 and AgNPs@Fe-EGCG + *S. aureus* eluted from the aforementioned membrane filter elements. Scale bar = 1 μm. (D) The SERS spectra of the aptamer-MBs + bacteria + SERS tags under the same conditions. Condition: 1 h for bacterial capture and 0.5 h for binding of SERS tags, measured with 532 nm laser (power: 12.5 mW), acquisition time 10 s. (E) SEM images of the binding complexes aptamer-MBs + *E. coli* O157: H7 + AgNPs@Fe-TA and aptamer-MBs + AgNPs@Fe-EGCG + *S. aureus*. Scale bar = 1 μm. (F) The ITC thermograms of the titration of a CWC suspension (200 μL, 1 × PBS buffer, pH 7.4) with a MPN solution (5.8 mM, 1 × PBS buffer, pH 7.4, 3 μL injections), measured at 25 °C.

shaking. After a reaction time of 1 h, the greyish-yellow product was washed once and concentrated 5 folds, which was finally stored at 4 °C in a refrigerator (BCD-539WT, Haier Group, Shandong, China) for further use.

2.4. Preparation of AgNPs@4-MB and AgNPs@4-MB@MPNs SERS tags

The AgNPs@4-MB SERS tag was obtained by adding 2.5 μL of 4-MB solution (0.1 M, DMSO solvent) into 1.5 mL of the above AgNPs solution, and incubated for 30 min under constant shaking at 1.6 *g*. The obtained solution was centrifuged (JW-3024HR, Anhui Jiawen Instrument and Equipment Industry Co., Ltd., Hefei, China) at 3663 *g* for 10 min to remove the excess 4-MB molecules before redispersion in water for further use.

To fabricate AgNPs@4-MB@MPNs SERS tags, 1.5 mL of the unmodified AgNPs solution was firstly diluted to 3.4 mL water before being added with 2.5 μL of 4-MB solution (0.1 M) under shaking. After 30 s of incubation, 50 μL of polyphenol solution (4 mg/mL, TA, EGCG, or GA) and 10 μL of metal salts solution (2 mg/mL of $FeCl_3 \cdot 6H_2O$, $Cu(NO_3)_2 \cdot 3H_2O$, or $ZrCl_4$) were sequentially added at (30 s interval) into the above mixture, followed with the addition of 15 μL of Na_2CO_3 (0.5 M) for another 5 min of shaking. The MPNs coated SERS tags were centrifuged, rinsed with water twice, and finally redispersed in 1 mL of water and stored at 4 °C for further use.

2.5. Conjunction of aptamers with NHS-MBs

In a typical experiment, 100 μL of NHS-MBs (10 mg/mL) was firstly washed with 500 μL of ice-cold hydrochloric acid (1 mM). Subsequently, 500 μL of PBS buffer containing 1.0 nmol of anti-bacteria aptamers (*anti-E. coli* O157: H7 or *anti-S. aureus*) was added to the beads and incubated under constant shaking at 1.6 *g* overnight at 4 °C. After that, the aptamer-modified MBs was separated and washed with 500 μL of ethanolamine (3 M) for several times before another incubation for 2 h with ethanolamine (3 M) to block non-specific sites on NHS-MBs. Finally, the aptamer-MBs was washed with PBS, redispersed in 1 mL of PBS (pH 7.4), and then stored at 4 °C for further use.

2.6. Bacterial cultivation

Two foodborne pathogens including Gram-positive (*S. aureus* (ATCC6538)) and Gram-negative (*E. coli* O157: H7 (ATCC700728)) bacteria were chosen as target bacteria, and *S. enterica* (ATCC14028)

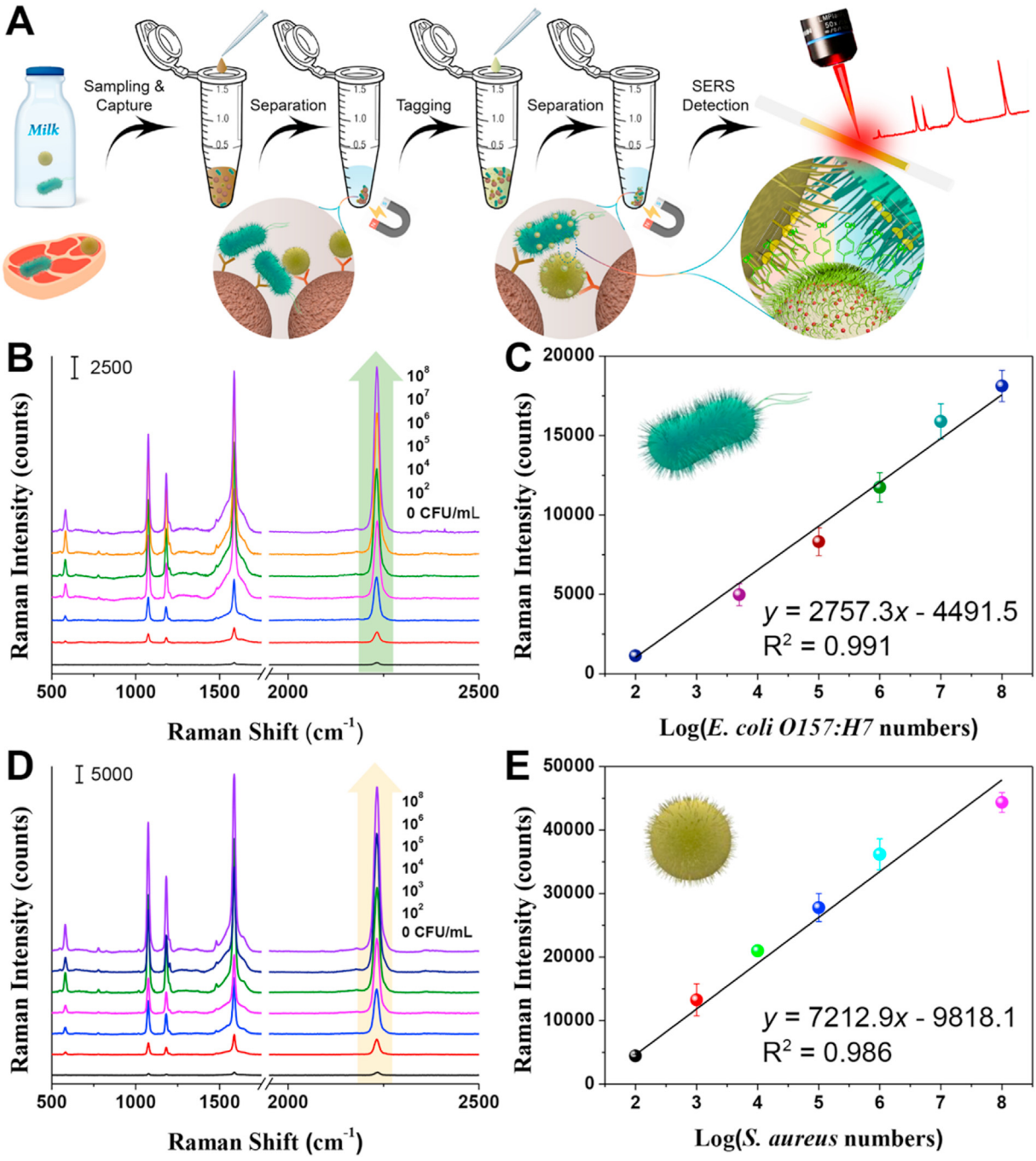

Fig. 3. (A) Schematic illustration of detecting foodborne bacteria with MPN-functionalized SERS tags. (B) The SERS spectra of the detection solution under different concentrations of *E. coli* O157: H7. (C) A calibration curve where the Raman intensity measured at 2231 cm^{-1} peak is plotted versus the logarithmic concentration of *E. coli* O157: H7. (D) The SERS spectra of the detection solution under different concentrations of *S. aureus*. (E) A calibration curve where the Raman intensity measured at 2231 cm^{-1} peak is plotted versus the logarithmic concentration of *S. aureus*. Condition: 1 h for bacterial capture and 0.5 h for binding of SERS tags, measured with 532 nm laser (power: 50 mW), acquisition time 10 s.

and *E. coli* (ATCC25922) were used as control. These strains were grown in both Luria-Bertani broth (LB) liquid culture media and agar plates. For liquid cultivation, the strains were cultured in 100 mL of LB media at 37 °C for several hours by constant shaking at 0.6 *g*. To prepare the targets for detection, the bacteria were cultured to log growth phase with OD_{600} of about 0.5. Viable counts of the bacterial colony-forming units (CFU) were determined by performing 20 μL of serial dilution of the bacterial culture plating on the solid LB agar media after incubation at 37 °C for 16 h. Meanwhile, the rest of the bacterial precipitates were centrifuged at 6511 *g* and washed with phosphate buffer saline (1 ×, pH 7.4) for several times. Bacterial cells were sequentially fixed with 90% (v/v) methanol for 10 min and with absolute methanol overnight in a refrigerator (BCD-539WT, Haier Group, Shandong, China) at −20 °C. All the bacteria were finally dispersed in absolute methanol at −20 °C, and an aliquot was rinsed with PBS before collection for detection.

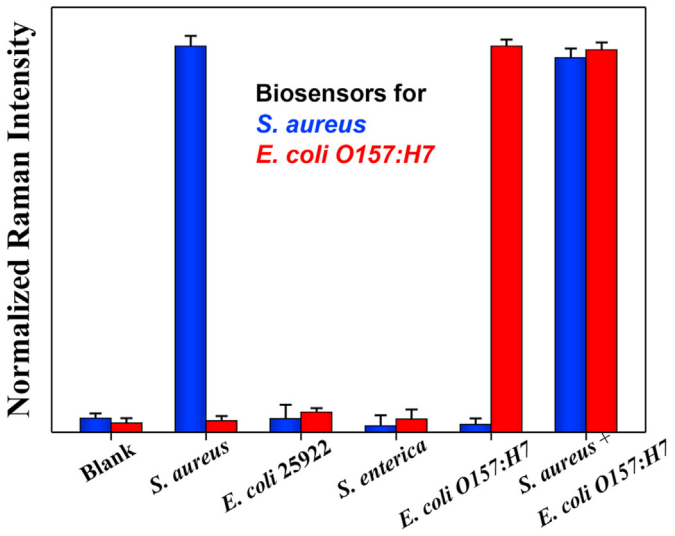

Fig. 4. Detection selectivity for target bacteria over common foodborne bacteria.

2.7. Detection procedures for foodborne bacteria

In a typical assay, 50 μL of aptamer-modified MBs was added to a 1.5 mL centrifuge tube. Subsequently, 50 μL of target bacteria suspension in different concentrations (10^1–10^8 CFU/mL) and 100 μL of PBS buffer were sequentially added. The mixture was incubated under constant shaking at 1.6 *g* and 37 °C for 1 h. The resulting bacteria-MBs complexes were magnetically separated by a magnetic separator rack (FMS096, Biyotime Biotechnology Ltd., Beijing, China) and rinsed three times with PBS to remove the excess free bacteria. After the washing procedure, the bacteria-MBs complexes were transferred in a new 1.5 mL centrifuge tube, and 100 μL of the above obtained SERS tags were incubated with the complexes for another 30 min at the same condition. The resulting aptamer-MBs/bacteria/Ag tags sandwich complexes were rinsed by water for three times before redispersion in 50 μL of pure water. Finally, 50 μL of the above aptamer-MBs/bacteria/Ag tags suspension was transferred to a capillary tube with an inner diameter of 1 mm for SERS measurements. In addition, the selectivity tests were performed similarly by replacing the target bacteria with the other bacteria.

2.8. Application to actual samples

To verify the applicability of AgNPs@MPNs tags, AgNPs@MPNs tags were used to detect *E. coli* O157: H7 or *S. aureus* in milk and beef samples. For the beef, 1.0 g of the meat was thoroughly crushed in 5.0 mL of 1 × PBS (pH 7.4) and kept in the refrigerator at 4 °C for 12 h. For the milk, 1 mL of the sample was fully mixed with 9.0 mL of PBS. Then, the supernatants were collected by centrifugation, followed by filtration through sterile syringe filters (0.22 μm, Aquosystem, Sangon Biotech Co., Ltd., Shanghai, China). These food suspensions were artificially inoculated with dilute bacterial culture to attain final concentrations of 1×10^3 and 1×10^6 CFU/mL, respectively. After gently shaking at 0.4 *g* and 37 °C for 2 h, the prepared solutions were taken as the analytes in the aforementioned detection protocol.

Table 1
Recent biosensors for the detection of pathogenic bacteria.

Analyte	Strategy and label	Recognizer	Detection parameter			Reference
			Time (min)	Interval (CFU/mL)	LOD (CFU/mL)	
E. coli O157: H7; *S. aureus*	SERS; AgNPs@4-MB@MPNs	MPNs	90	10^2–10^8 10^2–10^8	10^2 10^2	This work
Salmonella typhimurium	SERS; AuNPs@MBA/DSNB	antibodies	120	10^1–10^7	10^2 or 10^1	[62]
S. aureus	SERS combined laser induced breakdown spectroscopy; AgNPs	fingerprint	30	5×10^3–5×10^7	5×10^3	[63]
E. coli	SERS; Au@Ag core-shell nanorod	antibodies	210	10^2–10^7	10^2	[64]
E. coli; *S. aureus*	SERS microfluidic assay; silver island film	fingerprint	120	/	10^3	[65]
S. aureus	Colorimetric test strip; vancomycin modified AuNPs	vancomycin	125	/	10^9	[66]
Salmonella typhimurium	Multisignal lateral flow immunoassay; quantum dots-laden Fe_3O_4 NPs	antibodies	35	1.88×10^4 -1.88×10^7	Visual: 1.88×10^4; magnetic: 3.75×10^3; fluorescence: 3.75×10^3	[67]
E. coli B	Electrochemical; polyethylenimine-functionalized carbon nanotubes	bacteriophage	115	10^3–10^7	1.5×10^3	[4]
E. coli O157: H7	Electrochemical; Au@PtNPs-laden neutral red functionalized reduced graphene oxide	antibodies	105	8.9×10^3 -8.9×10^9	2.84×10^3	[68]

Table 2
Bacterial analysis in artificially contaminated food samples.

Analytes	Samples	Added mount (Log (CFU/mL))	Recovered mean[a] ± SD[b] (Log (CFU/mL))	Recovery (%)
E. coli O157: H7	Milk 1	3	2.49 ± 0.26	83.00
	Milk 2	6	6.33 ± 0.10	105.50
	Beef 1	3	3.20 ± 0.27	106.67
	Beef 2	6	5.81 ± 0.63	96.83
S. aureus	Milk 1	3	3.36 ± 0.15	112.00
	Milk 2	6	5.69 ± 0.51	94.83
	Beef 1	3	3.05 ± 0.69	101.67
	Beef 2	6	6.58 ± 0.18	109.67

[a] Mean of three determinations.
[b] SD: standard deviation.

2.9. Statistical analysis

All collected Raman spectra were processed with baseline correction using LabSpec 6 spectroscopy software suite (Horiba France SAS, Villeneuve d'Ascq, France). All measurements were conducted in triplicate and results were expressed as means ± standard deviation.

3. Results and discussion

3.1. Design and characterization of MPNs-encapsulated SERS tags

In a principle design, the multifunctional properties of polyphenolic chemistry were utilized to fabricate the well-refined silver SERS nanoagents. As depicted in Scheme 2, the polyphenolic compounds including TA, EGCG, and GA could be both rational reductant and antioxidant by virtue of their redox chemistry, enabling the reduction of silver nitrate into uniform AgNPs, while suppressing the self-oxidation of AgNPs in the environment. Further, the hydrophilic groups (*i.e.*, hydroxyl and carboxyl), residing on the surface of the AgNPs, could render the particles with good aqueous dispersity, which was conducive to the further adsorption and modification of mercapto reporter molecules. This process embodied the surface properties of polyphenolic chemistry. More importantly, metal-phenolic networking (coordination chemistry) between polyphenols and most of the metal ions ensured the functional encapsulation of silver SERS tags. Meanwhile, due to the affinity of polyphenols with many biomolecules, polyphenolic species could be designed as bioconjugation ligands for silver SERS tags. As such, metal-phenolic networks (MPNs) could be rationally constructed on the surface of SERS-active AgNPs, enabling not only protective encapsulation of silver SERS tags but targeted recognition of bacteria due to phenolic binding to bacterial cell wall components (CWCs) such as glycoproteins, lipopolysaccharides (LPS), peptidoglycans (PGs), etc.

In this study, uniform silver NPs were chosen for the fabrication of SERS tags, because they usually exhibit repeatedly higher SERS activity than that of other SERS-active noble-metal NPs. To actualize the polyphenolic synthesis of uniform silver SERS tags (Fig. 1A), a two-step seed growth synthesis was firstly achieved for the preparation of uniform and quasi-spherical AgNPs. Before seed growth, spherical silver seeds with a uniform size of about 27 nm was obtained by reducing $AgNO_3$ with TA under ambient condition (inset **i** of Fig. 1B), while the reduction of $AgNO_3$ with EGCG failed to generate regular Ag seeds (Fig. S1). To obtain a SERS-active silver core for AgNPs@MPNs SERS tag, the silver seeds were further grown to quasi-spherical AgNPs using polyphenolic reductant. As a result, the seeding growth using TA as reductant failed to generate regular AgNPs (Fig. S2A), while uniform and quasi-spherical AgNPs with a larger size of ~70 nm were obtained in the presence of EGCG (inset **ii** of Fig. 1B and Fig. S2B). Under similar conditions, the direct reaction of $AgNO_3$ with TA (Fig. S3A) or EGCG (Fig. S3B) in the absence of Ag seeds only resulted in irregular morphologies of AgNPs, which implied the necessity of seeding growth for regularly shaped AgNPs. As such, the simple and room-temperature preparation of regular AgNPs with potentially good SERS properties was achieved using TA and EGCG as green reductants sequentially.

On one hand, during SERS bioanalysis in complex food matrices, food carbohydrates, proteins and pigments usually generate obvious Raman background signals in the Raman shift range from 400 to 1800 cm^{-1}. To address this, 4-MB molecule, with a characteristic peak located in Raman-silent field (1800–2800 cm^{-1}), was employed as Raman reporter for the AgNP tags. On the other hand, conventional functionalization of Raman reporter molecules usually needs a couple of hours for efficient molecular adsorption and induces occasional aggregation of noble-metal NPs. Here, simultaneous encapsulation of 4-MB and surface functionalization of functional ligands was accomplished in minutes via the in-situ growth of MPNs on AgNPs surface in the presence of 4-MB (Fig. 1A). The SEM images in Fig. 1B (**iii**–**v**) indicated that metal-phenolic coordination of iron ions (III) with three polyphenols (TA, EGCG, and GA) succeeded in constructing MPNs-encapsulated monodisperse silver SERS tags. Further, the XRD diffractogram (Fig. 1C) of quasi-spherical AgNPs was consistent with the standard powder diffraction card of JCPDS No. 04–0783, which can be identified to AgNPs. Correspondingly, the TEM image of AgNPs@4-MB@Fe-TA, together with the Ag, Fe, C elemental distribution maps of the sample, confirmed the homogeneous distribution of MPNs layer on the AgNPs (Fig. 1D). Meanwhile, the UV–vis absorption spectra of these SERS tags were collected (Fig. 1E), and AgNPs and 4-MB modified AgNPs (AgNPs@4-MB) showed the same absorption peaks at 439 nm. However, compared with AgNPs and AgNPs@4-MB, slight redshifts of characteristic peaks occurred to the MPNs modified AgNPs samples, which consistently demonstrated the larger sizes of MPNs-coated tags (AgNPs@4-MB@MPNs). To examine the SERS properties of AgNPs@4-MB@MPNs, the SERS activities of AgNPs@4-MB@MPNs were compared with those of uncoated AgNPs@4-MB. As shown in Fig. 1F, all the tags showed obvious peaks at around 585, 783, 1078, 1181, 1586, and 2231 cm^{-1}, consistent with the characteristic SERS spectrum of 4-MB molecules. This result verified that 4-MB molecules were rapidly and efficiently adsorbed on AgNPs under the assistance of MPN encapsulation. Meanwhile, although not as high as the uncoated AgNPs@4-MB, the three AgNPs@4-MB@MPNs exhibited similarly high SERS activities and no interference peaks from MPN components under the same measurement conditions. Notably, the synthesis of AgNPs@4-MB@MPNs could be universal when using other metal ions like copper (II) and zirconium (IV) as building units (Fig. S4).

Meanwhile, the signal reproducibility of AgNPs@4-MB@MPNs was investigated. By measuring and mapping SERS signals of these colloidal tags at random positions of capillary tubes, the three AgNPs@4-MB@MPNs were confirmed to exhibit highly repeatable Raman intensities at a large selected focusing area (120 × 40 μm^2) (Fig. S5). Low relative standard deviations (RSD) of the Raman mapping results were achieved among 225 measurement spots of each tag, reaching RSD ranges of 5.04%–5.57% (@Fe-TA), 4.90%–7.30% (@Fe-EGCG), and 5.88%–7.85% (@Fe-GA), respectively. Besides high reproducibility, the anti-interference ability of SERS tag is crucial to its reliable performance in real sample conditions. Accordingly, the SERS performance of AgNPs@4-MB@MPNs was examined in the existence of some representative food ingredients (proteins, amino acids, carbohydrates, inorganic salts, and their mixtures). As shown in Fig. S6, although the spectral baselines became rugged after the addition of those food ingredients, the AgNPs@4-MB@MPNs showed acceptable changes with respect to peaks and peak intensities, especially for a characteristic peak at 2231 cm^{-1}. Moreover, the AgNPs@4-MB@MPNs nanostructures remained stable SERS activities in the ranged ionic strength (10–100 mM NaCl, Fig. S7A) and pH conditions (4–10, Fig. S7B). Thus, AgNPs@4-MB@MPNs tags were potentially workable in the analysis of real food samples. Furthermore, due to the protective encapsulation of MPNs, it was inspired to test the shelf stability of AgNPs@4-MB@MPNs tags, which is a key parameter for the commercialization of SERS tags. As a result, the relative SERS activities of three AgNPs@4-MB@MPNs tags (Fe-TA, Fe-EGCG, and Fe-GA) were largely maintained (~85%) during storage for 30 days in the refrigerator at 4 °C, whereas the unprotected AgNPs@4-MB tags suffered an obvious loss in relative SERS activity during the same shelf condition (Fig. 1G). That is, MPNs coatings could stabilize SERS

tags to render a much longer shelf life. These results evidenced that with the inspiration of polyphenolic chemistry, uniform, monodisperse, interference-free, reproducible, and shelf-stable SERS tags were obtained.

3.2. Bacterial recognition via AgNPs@4-MB@MPNs tags

Recent studies have elaborated the close interactions between polyphenol derivatives (including MPNs) and bacterial CWCs [53-56,59,60], which implies the possibility of polyphenol-guest binding in use for bacterial targeting. To make use of the as-prepared polyphenolic SERS tags, our further attention was thrown upon the possible affinity of MPNs to bacterial CWCs. Firstly, Raman spectra were acquired to investigate the incubation of bacteria with AgNPs or AgNPs@MPNs (without 4-MB modification) in PBS buffer (pH 7.4), respectively. As shown in Fig. 2A, besides the existence of spectral information from the polyphenolic residual groups, negligible decreases in Raman intensity were observed for AgNPs (**inset i**) before/after incubation with *E. coli* O157: H7 or *S. aureus*, which preliminarily ruled out the possible interactions between AgNPs and these bacterial cells. In contrast, MPNs functionalized AgNPs (@Fe-TA, @Fe-EGCG and AgNPs@Fe-GA shown in **insets ii, iii, and iv, respectively**) display distinguishable SERS responses to the presence of bacterial cells. As can be seen, both *E. coli* O157: H7 and *S. aureus* induced sharp decrease of Raman spectra of AgNPs@MNPs, and the regions located at around 731, 1340, 1955 cm^{-1} displayed unique features in spectra compared with those of AgNPs@MNPs alone. The Raman spectral analysis initially implied intense interactions of AgNPs@MNPs with bacteria cells. In addition, the solutions of bacteria cells, AgNPs/AgNPs@MNPs, and their incubations were filtered with the syringe filters, where the filtrate components were analyzed by UV−vis spectra. Due to size effects, *E. coli* O157: H7 (Fig. S8A) with an average size of $1 \times 2-3$ μm and *S. aureus* (Fig. S8B) with an average diameter of 1.2 μm were validated to be detained upon the syringe filtering, showing no characteristic absorbance at OD_{600} of the filtrates. In comparison, the solutions of AgNPs and AgNPs@MPNs (<100 nm) were found to smoothly penetrate through the filters, resulting in negligible decreases of characteristic absorbance at OD_{445} (Fig. 2B). More importantly, the solutions of bacteria/AgNPs mixture remained almost unchanged in absorbance before/after filtration, while incubation of AgNPs@MPNs (Fe-TA, Fe-EGCG, and Fe-GA) with either *E. coli* O157: H7 or *S. aureus* cells contributed to dramatically lower the characteristic absorbance of these solutions. These results suggested that AgNPs were free in incubation solution, thus permeable during the filtration, while AgNPs@MPNs were largely retained due to that they existed in the form of AgNPs@MPNs/bacterial cells complex. Moreover, when eluting the retention components of AgNPs@MPNs/bacteria incubation solutions from the filters, the intense binding of AgNPs@MPNs to *E. coli* O157: H7 or *S. aureus* cells could be facilely visualized via the SEM images (Fig. 2C), showing that the AgNPs@MPNs particles were densely attached on the surface of bacterial cells. This evidence proved that MPN ligands could be a non-specific bio-recognizer for targeting both Gram-positive (*S. aureus*) and Gram-negative (*E. coli* O157: H7) bacterial cells, launching AgNPs@4-MB@MPNs as a robust candidate of SERS tags for probing foodborne bacteria.

Thereafter, efforts were devoted to the selection of suitable polyphenolic SERS tags for specific bacteria. To realize this, magnetic beads (MBs, ~2 μm) modified with *anti*-analyte aptamer ligands (Fig. S9) were used as capture probe for *E. coli* O157: H7 and *S. aureus*, respectively. Typically, the target bacteria (10^8 CFU/mL) in PBS buffer were firstly incubated with aptamer-modified MBs and sequentially reacted with AgNPs@4-MB@MPNs after magnetic separation and washing. As such, the sandwiched complexes of aptamer-MBs/bacteria/AgNPs@4-MB@MPNs, after separation and redispersion, could be obtained (if present) for the choice of suitable tags via SERS measurements. As shown in Fig. 2D, AgNPs@4-MB@Fe-TA tag resulted in much higher SERS peaks for probing *E. coli* O157: H7 over the other two tags, while the binding sandwich of aptamer-MBs/*S. aureus*/AgNPs@4-MB@Fe-EGCG showed the best SERS signal among the three under the same conditions. Accordingly, the corresponding SEM analysis (Fig. 2E) confirmed that *E. coli* O157: H7 and *S. aureus* could be efficiently sandwiched between aptamer modified MBs and MPNs encapsulated SERS tags.

To investigate the possible mechanisms behind, it was assumed that the targeting ability of AgNPs@4-MB@MPNs for bacteria could be mainly attributed to the interactions between MPN ligands and bacterial CWCs. For common bacteria such as *E. coli* O157: H7 and *S. aureus*, CWCs contain mainly LPS (Gram-negative) and PG (Gram-positive), followed with teichoic-acid (Gram-positive), membrane proteins, and lipids. Several previous studies proved that polyphenolic compounds could inherently bind to proteins [52,54], demonstrating the membrane proteins as target sites for polyphenolic recognizers. Besides, as the main CWCs, LPS and PG have potential to present intense interactions with polyphenols [59]. The fact that bacterial cells of *E. coli* O157: H7 or *S. aureus* are negatively charged in pH-neutral solution, together with the negative surface charges of MPNs encapsulated silver tags revealed by the zeta potential results (Fig. S10), eliminated the possibility of electrostatic interactions between MPNs and CWCs. To clarify this, isothermal titration micro-calorimetry (ITC) was conducted to analyze the interactions of MPNs and bacterial CWCs (LPS and PG) in PBS buffer (10 mM, pH 7.4) [50,61]. As displayed in Fig. 2F, by allowing MPNs to titrate bacterial CWCs, dramatic heat changes occurred with a decreasing tendency, as anticipated if MPN (Fe-TA and Fe-EGCG) ligands could chemically bind to LPS and PG. In comparison, negligible heat changes could be measured during the titration of PBS buffer with MPNs solution (Fig. S11). Correspondingly, the integrated heat changes were plotted against [MPNs]/[CWC] molar ratio (Fig. S12), indicating exclusively endothermic reactions between MPNs and LPS/PG. Thus, it was reasonable to conclude that polyphenolic chemistry could endow AgNPs@4-MB@MPNs tags with bacterial binding affinity via the multiplex chemical interactions between MPNs and CWCs including LPS, PG, and possibly proteins.

3.3. Detection of foodborne bacteria via AgNPs@4-MB@MPNs tags

Based on the above results, AgNPs@4-MB@MPNs are promising to be high-performance SERS tags for the rapid and reliable screening of foodborne pathogens. Accordingly, AgNPs@4-MB@Fe-TA and AgNPs@4-MB@Fe-EGCG were chosen to target *E. coli* O157: H7 and *S. aureus*, respectively. As illustrated in Fig. 3A, the detection started with capturing target bacteria from food samples using aptamer-modified MBs (capture probe), sequentially the separation and washing procedures, and then incubation with MPNs functionalized SERS tags (detection probe), where the SERS tags could densely bind to bacterial CWCs. After secondary separation and washing procedures, the formed sandwich structures (capture probe@bacteria@SERS tag) could be eventually measured in a capillary tube using SERS spectra. As such, bacterial detection with this SERS biosensor could be accomplished within 1.5 h based on the use of cheap and easily available recognizers (aptamers/MPNs).

To evaluate the sensitivity for detecting *E. coli* O157: H7, different concentrations of *E. coli* O157: H7 ($0-10^8$ CFU/mL) were measured under the optimal conditions. As shown in Fig. 3B, the SERS spectral peaks of the detection solution increased with increasing the *E. coli* cell concentrations, while almost no peaks were observed in the absence of *E. coli* O157: H7. By fitting the

Raman intensity at 2231 cm^{-1} (Raman-silent peak) with a logarithmic concentration of *E. coli* O157: H7 (Fig. 3C), the linear equation of $y = 2757.3x - 4495.1$ ($R^2 = 0.991$) with a broad concentration range (10^2–10^8) was obtained. The limit of detection (LOD) was calculated by the $3\sigma/S$ principle, where σ = standard deviation of blank and S = slope of calibration curve. The calculated LOD is 2.6 CFU/mL, which resides below the linear range, where the calibration curve is no longer valid. Therefore, we adopted the smallest concentration of bacteria that can be actually detected as a more conservative estimation value of LOD for this method, which was 10^2 CFU/mL in a 50 μL E. *coli* O157: H7 volume. Similarly, sensitive responses of AgNPs@4-MB@Fe-EGCG tags at 2231 cm^{-1} were recorded *versus* the varied concentrations of *S. aureus* in the detection solutions (Fig. 3D). A good linear correlation ($R^2 = 0.986$) in the range of 10^2–10^8 CFU/mL was obtained (Fig. 3E), reaching an actual LOD as low as 10^2 CFU/mL for *S. aureus*. Thereafter, the specificity and anti-interference capability of this SERS biosensor were evaluated by using common foodborne bacteria such as *E. coli* (ATCC22922), and *S. enterica* (ATCC14028). As shown in Fig. 4, strong SERS signal of the biosensor for *S. aureus* occurred in the presence of *S. aureus* cells, while only weak background signals were detected in the presence of *E. coli* 25922, *S. enterica, or E. coli* O157: H7. Meanwhile, the SERS biosensor for *E. coli* O157: H7 responded strongly to the presence of *E. coli* O157: H7, but not to other bacteria. In addition, this SERS biosensor performed well in the coexistence of target bacteria and interfering bacteria.

In addition, Table 1 gives a comparison of this biosensor with other recent biosensing methods, indicating that this biosensor is highly competitive over the listed methods in terms of their recognition patterns and detection parameters (assay time, intervals, and LODs). Therefore, polyphenolic chemistry derived SERS tags are demonstrated to empower cost-efficient, robust, and reliable SERS biosensors for foodborne pathogens.

3.4. Detection of real food samples

To test the workability of the polyphenolic SERS tags in real food samples, further detection was conducted for foodborne bacteria in milk and beef samples, and results are listed in Table 2, indicating that this SERS biosensor could perform well in both milk and beef samples with recoveries from 83.00 to 106.67% for *E. coli* O157: H7 and recoveries from 94.83 to 112.00% for *S. aureus*, respectively. Therefore, the obtained results validated that polyphenolic SERS tags based biosensors can be a robust candidate for monitoring microbial food safety.

4. Conclusions

The current study confirmed the possibility of polyphenolic chemistry for the green synthesis of reproducible and durable SERS tags for non-specific targeting and sensing of foodborne bacteria. Using the multivariate chemistry of polyphenolic compounds, 4-MB modified quasi-spherical silver nanotags with a coating of MPNs (Fe-TA, Fe-EGCG, Fe-GA, Zr-TA, and Cu-TA) were successfully obtained. The polyphenolic SERS nanotags (AgNPs@4-MB@MPNs) were validated to be reproducible, shelf-stable (workable in one month), and interference-free, which overpassed most of previously reported silver nanotags. Notably, MPNs were demonstrated to be an emerging artificial bio-recognizer for the non-selective targeting of G+/G-bacteria such as *E. coli* and *S. aureus*, which was largely attributed to the intensive interactions between the polyphenolic groups and bacterial CWCs. By taking advantages of the aforementioned merits of polyphenolic SERS nanotags, a sensitive and cost-efficient SERS biosensor for foodborne bacteria was thus proposed based on the sandwich recognition of aptamer-functionalized magnetic beads and polyphenolic SERS nanotags. The performance of this method was well validated by the comparable detection results among others and the test in real food samples (recoveries ranging from 83.00% to 112.00%). Future work is encouraged to involve more functional polyphenolic derivatives in the synthesis, functionalization, and customization of bioaffinity SERS nanotags.

Author statement

Lunjie Huang: Writing – original draft, Formal analysis, Investigation. Da-Wen Sun: Supervision, Funding acquisition, Resources, Writing – review & editing. Zhihui Wu: Investigation. Hongbin Pu: Validation, Funding acquisition, Resources. Qingyi Wei: Resources.

Declaration of competing interest

The authors declare that they have no known competing financial interests or personal relationships that could have appeared to influence the work reported in this paper.

Acknowledgments

The authors are grateful to the National Key R&D Program of China (2018YFC1603400) for its support. This research was also supported by the Guangdong Basic and Applied Basic Research Foundation (2020A1515010936), the Fundamental Research Funds for the Central Universities (D2190450), the Contemporary International Collaborative Research Center of Guangdong Province on Food Innovative Processing and Intelligent Control (2019A050519001) and the Common Technical Innovation Team of Guangdong Province on Preservation and Logistics of Agricultural Products (2020KJ145).

Appendix A. Supplementary data

Supplementary data to this article can be found online at https://doi.org/10.1016/j.aca.2021.338570.

References

[1] D. Laborde, W. Martin, J. Swinnen, R. Vos, COVID-19 risks to global food security, Science 369 (6503) (2020) 500–502.
[2] L. Huang, D.-W. Sun, H. Pu, Q. Wei, Development of nanozymes for food quality and safety detection: principles and recent applications, Compr. Rev. Food Sci. Food Saf. 18 (5) (2019) 1496–1513.
[3] L. Huang, D.-W. Sun, H. Pu, Q. Wei, L. Luo, J. Wang, A colorimetric paper sensor based on the domino reaction of acetylcholinesterase and degradable γ-MnOOH nanozyme for sensitive detection of organophosphorus pesticides, Sens. Actuator B: Chem. 290 (2019) 573–580.
[4] Y. Zhou, A. Marar, P. Kner, R.P. Ramasamy, Charge-directed immobilization of bacteriophage on nanostructured electrode for whole-cell electrochemical biosensors, Anal. Chem. 89 (11) (2017) 5734–5741.
[5] D.D. Galvan, V. Parekh, E. Liu, E.L. Liu, Q. Yu, Sensitive bacterial detection via dielectrophoretic-enhanced mass transport using surface-plasmon-resonance biosensors, Anal. Chem. 90 (24) (2018) 14635–14642.
[6] X. Zhou, H. Pu, D.-W. Sun, DNA functionalized metal and metal oxide nanoparticles: principles and recent advances in food safety detection, Crit. Rev. Food Sci. Nutr. (2020) 1–20.
[7] J.H. Granger, N.E. Schlotter, A.C. Crawford, M.D. Porter, Prospects for point-of-care pathogen diagnostics using surface-enhanced Raman scattering (SERS), Chem. Soc. Rev. 45 (14) (2016) 3865–3882.
[8] D.-W. Sun, L. Huang, H. Pu, J. Ma, Introducing reticular chemistry into agrochemistry, Chem. Soc. Rev. 50 (2) (2021) 1070–1110.
[9] J. Langer, D. Jimenez de Aberasturi, J. Aizpurua, R.A. Alvarez-Puebla, B. Auguie, J.J. Baumberg, G.C. Bazan, S.E.J. Bell, A. Boisen, A.G. Brolo, J. Choo, D. Cialla-May, V. Deckert, L. Fabris, K. Faulds, F.J. Garcia de Abajo, R. Goodacre, D. Graham, A.J. Haes, C.L. Haynes, C. Huck, T. Itoh, M. Kall, J. Kneipp, N.A. Kotov, H. Kuang, E.C. Le Ru, H.K. Lee, J.F. Li, X.Y. Ling, S.A. Maier, T. Mayerhofer, M. Moskovits, K. Murakoshi, J.M. Nam, S. Nie, Y. Ozaki, I. Pastoriza-Santos, J. Perez-Juste, J. Popp, A. Pucci, S. Reich, B. Ren, G.C. Schatz, T. Shegai, S. Schlucker, L.L. Tay, K.G. Thomas, Z.Q. Tian, R.P. Van Duyne, T. Vo-Dinh, Y. Wang, K.A. Willets,

C. Xu, H. Xu, Y. Xu, Y.S. Yamamoto, B. Zhao, L.M. Liz-Marzan, Present and future of surface-enhanced Raman scattering, ACS Nano 14 (1) (2020) 28–117.
[10] D. Zhang, H. Pu, L. Huang, D.-W. Sun, Advances in flexible surface-enhanced Raman scattering (SERS) substrates for nondestructive food detection: Fundamentals and recent applications, Trends Food Sci. Technol. 109 (2021) 690–701.
[11] B. Hu, H. Pu, D.-W. Sun, Multifunctional cellulose based substrates for SERS smart sensing: Principles, applications and emerging trends for food safety detection, Trends Food Sci. Technol. 110 (2021) 304–320.
[12] B. Hu, D.-W. Sun, H. Pu, Q. Wei, A dynamically optical and highly stable pNIPAM @ Au NRs nanohybrid substrate for sensitive SERS detection of malachite green in fish fillet, Talanta 218 (2020) 121188.
[13] B. Hu, D.-W. Sun, H. Pu, Q. Wei, Rapid nondestructive detection of mixed pesticides residues on fruit surface using SERS combined with self-modeling mixture analysis method, Talanta 217 (2020) 120998.
[14] L. Wu, H. Pu, L. Huang, D.-W. Sun, Plasmonic nanoparticles on metal-organic framework: A versatile SERS platform for adsorptive detection of new coccine and orange II dyes in food, Food Chem 328 (2020) 127105.
[15] A. Hussain, D.-W. Sun, H. Pu, SERS detection of urea and ammonium sulfate adulterants in milk with coffee ring effect, Food Addit. Contam. A 36 (6) (2019) 851–862.
[16] W. Zhang, J. Ma, D.-W. Sun, Raman spectroscopic techniques for detecting structure and quality of frozen foods: principles and applications, Crit. Rev. Food Sci. Nutr. (2020) 1–17.
[17] D. Li, Z. Zhu, D.-W. Sun, Visualization of the in situ distribution of contents and hydrogen bonding states of cellular level water in apple tissues by confocal Raman microscopy, Analyst 145 (3) (2020) 897–907.
[18] Y. Wang, B. Yan, L. Chen, SERS tags: novel optical nanoprobes for bioanalysis, Chem. Rev. 113 (3) (2013) 1391–1428.
[19] Z. Wu, H. Pu, D.-W. Sun, Fingerprinting and tagging detection of mycotoxins in agri-food products by surface-enhanced Raman spectroscopy: Principles and recent applications, Trends Food Sci. Technol. 110 (2021) 393–404.
[20] H. He, D.-W. Sun, H. Pu, L. Huang, Bridging Fe3O4@Au nanoflowers and Au@Ag nanospheres with aptamer for ultrasensitive SERS detection of aflatoxin B1, Food Chem 324 (2020) 126832.
[21] X. Zhou, Z. Hu, D. Yang, S. Xie, Z. Jiang, R. Niessner, C. Haisch, H. Zhou, P. Sun, Bacteria detection: from powerful SERS to its advanced compatible techniques, Adv. Sci. 7 (23) (2020) 2001739.
[22] K. Wang, D.-W. Sun, H. Pu, Q. Wei, Polymer multilayers enabled stable and flexible Au@Ag nanoparticle array for nondestructive SERS detection of pesticide residues, Talanta 223 (2021) 121782.
[23] K. Wang, D.-W. Sun, H. Pu, Q. Wei, Surface-enhanced Raman scattering of core-shell Au@Ag nanoparticles aggregates for rapid detection of difenoconazole in grapes, Talanta 191 (2019) 449–456.
[24] K. Wang, D.-W. Sun, H. Pu, Q. Wei, Shell thickness-dependent Au@Ag nanoparticles aggregates for high-performance SERS applications, Talanta 195 (2019) 506–515.
[25] N. Hussain, H. Pu, A. Hussain, D.-W. Sun, Rapid detection of ziram residues in apple and pear fruits by SERS based on octanethiol functionalized bimetallic core-shell nanoparticles, Spectrochim. Acta A 236 (2020) 118357.
[26] A. Hussain, H. Pu, D.-W. Sun, SERS detection of sodium thiocyanate and benzoic acid preservatives in liquid milk using cysteamine functionalized core-shelled nanoparticles, Spectrochim. Acta Part A 229 (2020) 117994.
[27] A. Hussain, H. Pu, B. Hu, D.-W. Sun, Au@Ag-TGANPs based SERS for facile screening of thiabendazole and ferbam in liquid milk, Spectrochim. Acta Part A 245 (2021) 118908.
[28] L. Xing, Y. Xiahou, P. Zhang, W. Du, H. Xia, Size control synthesis of monodisperse, quasi-spherical silver nanoparticles to realize surface-enhanced Raman scattering uniformity and reproducibility, ACS Appl. Mater. Interfaces 11 (19) (2019) 17637–17646.
[29] K. Wang, D.-W. Sun, H. Pu, Q. Wei, Two-dimensional Au@Ag nanodot array for sensing dual-fungicides in fruit juices with surface-enhanced Raman spectroscopy technique, Food Chem 310 (2020) 125923.
[30] N. Hussain, H. Pu, D.-W. Sun, Core size optimized silver coated gold nanoparticles for rapid screening of tricyclazole and thiram residues in pear extracts using SERS, Food Chem 350 (2021) 129025.
[31] A. Hussain, D.-W. Sun, H. Pu, Bimetallic core shelled nanoparticles (Au@AgNPs) for rapid detection of thiram and dicyandiamide contaminants in liquid milk using SERS, Food Chem 317 (2020) 126429.
[32] K. Wang, D.-W. Sun, H. Pu, Q. Wei, A rapid dual-channel readout approach for sensing carbendazim with 4-aminobenzenethiol-functionalized core–shell Au@Ag nanoparticles, Analyst 145 (5) (2020) 1801–1809.
[33] S. Ma, Q. Li, Y. Yin, J. Yang, D. Liu, Interference-free surface-enhanced Raman scattering tags for single-cell molecular imaging with a high signal-to-background ratio, Small 13 (15) (2017).
[34] H. Kang, J.T. Buchman, R.S. Rodriguez, H.L. Ring, J. He, K.C. Bantz, C.L. Haynes, Stabilization of silver and gold nanoparticles: Preservation and improvement of plasmonic functionalities, Chem. Rev. 119 (1) (2019) 664–699.
[35] B. Mir-Simon, I. Reche-Perez, L. Guerrini, N. Pazos-Perez, R.A. Alvarez-Puebla, Universal one-pot and scalable synthesis of SERS encoded nanoparticles, Chem. Mater. 27 (3) (2015) 950–958.
[36] Q. Yu, Y. Wang, R. Mei, Y. Yin, J. You, L. Chen, Polystyrene encapsulated SERS tags as promising standard tools: simple and universal in synthesis; highly sensitive and ultrastable for bioimaging, Anal. Chem. 91 (8) (2019) 5270–5277.
[37] K. Wang, D.-W. Sun, H. Pu, Q. Wei, L. Huang, Stable, flexible, and high-performance SERS chip enabled by a ternary film-packaged plasmonic nanoparticle array, ACS Appl. Mater. Interfaces 11 (32) (2019) 29177–29186.
[38] J. Chen, S.M. Andler, J.M. Goddard, S.R. Nugen, V.M. Rotello, Integrating recognition elements with nanomaterials for bacteria sensing, Chem. Soc. Rev. 46 (5) (2017) 1272–1283.
[39] V.M. Szlag, R.S. Rodriguez, J. He, N. Hudson-Smith, H. Kang, N. Le, T.M. Reineke, C.L. Haynes, Molecular affinity agents for intrinsic surface-enhanced Raman scattering (SERS) sensors, ACS Appl. Mater. Interfaces 10 (38) (2018) 31825–31844.
[40] H. Jayan, H. Pu, D.-W. Sun, Recent development in rapid detection techniques for microorganism activities in food matrices using bio-recognition: a review, Trends Food Sci. Technol. 95 (2020) 233–246.
[41] K. Yuan, Q. Mei, X. Guo, Y. Xu, D. Yang, B.J. Sanchez, B. Sheng, C. Liu, Z. Hu, G. Yu, H. Ma, H. Gao, C. Haisch, R. Niessner, Z. Jiang, Z. Jiang, H. Zhou, Antimicrobial peptide based magnetic recognition elements and Au@Ag-GO SERS tags with stable internal standards: a three in one biosensor for isolation, discrimination and killing of multiple bacteria in whole blood, Chem. Sci. 9 (47) (2018) 8781–8795.
[42] H. Wang, Y. Zhou, X. Jiang, B. Sun, Y. Zhu, H. Wang, Y. Su, Y. He, Simultaneous capture, detection, and inactivation of bacteria as enabled by a surface-enhanced Raman scattering multifunctional chip, Angew. Chem. Int. Ed. 54 (17) (2015) 5132–5136.
[43] D. Lin, T. Qin, Y. Wang, X. Sun, L. Chen, Graphene oxide wrapped SERS tags: multifunctional platforms toward optical labeling, photothermal ablation of bacteria, and the monitoring of killing effect, ACS Appl. Mater. Interfaces 6 (2) (2014) 1320–1329.
[44] T.Y. Liu, K.T. Tsai, H.H. Wang, Y. Chen, Y.H. Chen, Y.C. Chao, H.H. Chang, C.H. Lin, J.K. Wang, Y.L. Wang, Functionalized arrays of Raman-enhancing nanoparticles for capture and culture-free analysis of bacteria in human blood, Nat. Commun. 2 (2011) 538.
[45] Y.Q. Li, B. Zhu, Y. Li, W.R. Leow, R. Goh, B. Ma, E. Fong, M. Tang, X. Chen, A synergistic capture strategy for enhanced detection and elimination of bacteria, Angew. Chem. Int. Ed. 53 (23) (2014) 5837–5841.
[46] L.F. Tadesse, C.S. Ho, D.H. Chen, H. Arami, N. Banaei, S.S. Gambhir, S.S. Jeffrey, A.A.E. Saleh, J. Dionne, Plasmonic and electrostatic interactions enable uniformly enhanced liquid bacterial surface-enhanced Raman scattering (SERS), Nano Lett. 20 (10) (2020) 7655–7661.
[47] T. Bu, J. Wang, L. Huang, L. Dou, B. Zhao, T. Li, D. Zhang, New functional tracer-two-dimensional nanosheet-based immunochromatographic assay for Salmonella enteritidis detection, J. Agric. Food Chem. 67 (23) (2019) 6642–6649.
[48] H. Ejima, J.J. Richardson, F. Caruso, Metal-phenolic networks as a versatile platform to engineer nanomaterials and biointerfaces, Nano Today 12 (2017) 136–148.
[49] Y. Yoda, Z.Q. Hu, W.H. Zhao, T. Shimamura, Different susceptibilities of Staphylococcus and Gram-negative rods to epigallocatechin gallate, J. Infect. Chemother. 10 (1) (2004) 55–58.
[50] J. Howe, J. Andra, R. Conde, M. Iriarte, P. Garidel, M.H. Koch, T. Gutsmann, I. Moriyon, K. Brandenburg, Thermodynamic analysis of the lipopolysaccharide-dependent resistance of gram-negative bacteria against polymyxin B, Biophys. J. 92 (8) (2007) 2796–2805.
[51] M.E. Rhodes, The cytology of Pseudomonas spp. as revealed by a silver-plating staining method, Microbiology 18 (3) (1958) 639–648.
[52] S. Shi, W. Zhang, X. Ren, M. Li, J. Sun, G. Li, Y. Wang, T. Yue, J. Wang, An advanced and universal method to high-efficiently deproteinize plant polysaccharides by dual-functional tannic acid-fe(III) complex, Carbohydr. Polym. 226 (2019) 115283.
[53] J.B. Delehanty, B.J. Johnson, T.E. Hickey, T. Pons, F.S. Ligler, Binding and neutralization of lipopolysaccharides by plant proanthocyanidins, J. Nat. Prod. 70 (11) (2007) 1718–1724.
[54] B.L. Tardy, J.J. Richardson, V. Nithipipat, K. Kempe, J. Guo, K.L. Cho, M.A. Rahim, H. Ejima, F. Caruso, Protein adsorption and coordination-based end-tethering of functional polymers on metal-phenolic network films, Biomacromolecules 20 (3) (2019) 1421–1428.
[55] G. Yun, J.J. Richardson, M. Capelli, Y. Hu, Q.A. Besford, A.C.G. Weiss, H. Lee, I.S. Choi, B.C. Gibson, P. Reineck, F. Caruso, The biomolecular corona in 2D and reverse: patterning metal–phenolic networks on proteins, lipids, nucleic acids, polysaccharides, and fingerprints, Adv. Funct. Mater. 30 (1) (2019).
[56] L.N. Silva, K.R. Zimmer, A.J. Macedo, D.S. Trentin, Plant natural products targeting bacterial virulence factors, Chem. Rev. 116 (16) (2016) 9162–9236.
[57] W. Wu, J. Zhang, M. Zheng, Y. Zhong, J. Yang, Y. Zhao, W. Wu, W. Ye, J. Wen, Q. Wang, J. Lu, An aptamer-based biosensor for colorimetric detection of Escherichia coli O157:H7, PloS One 7 (11) (2012), e48999.
[58] X. Cao, S. Li, L. Chen, H. Ding, H. Xu, Y. Huang, J. Li, N. Liu, W. Cao, Y. Zhu, B. Shen, N. Shao, Combining use of a panel of ssDNA aptamers in the detection of Staphylococcus aureus, Nucleic Acids Res. 37 (14) (2009) 4621–4628.
[59] X. Liu, C. Le Bourvellec, C.M.G.C. Renard, Interactions between cell wall polysaccharides and polyphenols: effect of molecular internal structure, Compr. Rev. Food Sci. Food Saf. 19 (6) (2020) 3574–3617.
[60] W. Zhang, Q.A. Besford, A.J. Christofferson, P. Charchar, J.J. Richardson, A. Elbourne, K. Kempe, C.E. Hagemeyer, M.R. Field, C.F. McConville, I. Yarovsky, F. Caruso, Cobalt-directed assembly of antibodies onto metal-phenolic networks for enhanced particle targeting, Nano Lett. 20 (4) (2020) 2660–2666.
[61] O. Callies, A. Hernandez Daranas, Application of isothermal titration

calorimetry as a tool to study natural product interactions, Nat. Prod. Rep. 33 (7) (2016) 881–904.
[62] S. Chattopadhyay, P.K. Sabharwal, S. Jain, A. Kaur, H. Singh, Functionalized polymeric magnetic nanoparticle assisted SERS immunosensor for the sensitive detection of S. typhimurium, Anal. Chim. Acta 1067 (2019) 98–106.
[63] W. Liao, Q. Lin, S. Xie, Y. He, Y. Tian, Y. Duan, A novel strategy for rapid detection of bacteria in water by the combination of three-dimensional surface-enhanced Raman scattering (3D SERS) and laser induced breakdown spectroscopy (LIBS), Anal. Chim. Acta 1043 (2018) 64–71.
[64] L. Bi, X. Wang, X. Cao, L. Liu, C. Bai, Q. Zheng, J. Choo, L. Chen, SERS-active Au@Ag core-shell nanorod (Au@AgNR) tags for ultrasensitive bacteria detection and antibiotic-susceptibility testing, Talanta 220 (2020) 121397.
[65] H.-K. Huang, H.-W. Cheng, C.-C. Liao, S.-J. Lin, Y.-Z. Chen, J.-K. Wang, Y.-L. Wang, N.-T. Huang, Bacteria encapsulation and rapid antibiotic susceptibility test using a microfluidic microwell device integrating surface-enhanced Raman scattering, Lab Chip 20 (14) (2020) 2520–2528.
[66] Q. You, X. Zhang, F.-G. Wu, Y. Chen, Colorimetric and test stripe-based assay of bacteria by using vancomycin-modified gold nanoparticles, Sensor. Actuator. B Chem. 281 (2019) 408–414.
[67] J. Hu, Y.-Z. Jiang, M. Tang, L.-L. Wu, H.-y. Xie, Z.-L. Zhang, D.-W. Pang, Colorimetric-fluorescent-magnetic nanosphere-based multimodal assay platform for Salmonella detection, Anal. Chem. 91 (1) (2019) 1178–1184.
[68] X. Mo, Z. Wu, J. Huang, G. Zhao, W. Dou, A sensitive and regenerative electrochemical immunosensor for quantitative detection of Escherichia coli O157:H7 based on stable polyaniline coated screen-printed carbon electrode and rGO-NR-Au@Pt, Anal. Methods 11 (11) (2019) 1475–1482.